FULL PAPER

Application of response surface methodology on efficiency of fig leaf activated carbon for removal of methylene blue dye

Safaa Talib Al-Asadi | **Fouad Fadhil Al-Qaim***

Department of Chemistry, College of Science for Women, University of Babylon, Hillah, Iraq

Fig leaves that have fallen off the tree are a common agricultural waste in Iraq. In this study, a very common used dye methylene blue (MB), was tested to be removed using a low-adsorbent "fig leaves activated carbon, FGAC" from its solution. Scanner electron microscopy (SEM) and Fourier transform infrared spectroscopy (FTIR) were used to characterize the adsorbent. The effects of quantity of activated carbon, the concentration of methylene blue, the pH of solution, and the length of agitation were investigated using response surface methodology software. The studied variables included the amount of activated carbon (0.02-0.1 g), methylene blue dye concentration levels (20-100 mg/L), sample solution (25-100 mL), pH solution (4-11), carbonization temperature (150 °C-550 °C), and contact time (20-60 min). The Analysis of Variance was investigated to test the model's efficacy. The greatest MB removal efficiency was achieved by combining the effects of activated carbon quantity and solution pH, activated carbon amount, agitation time, pH solution, and agitation duration. Several contemporaneous interactions produced less striking outcomes. To achieve 99.5% high removal efficiency for MB under ideal conditions, the ideal activated carbon amount, methylene blue concentration, contact time, pH solution, sample volume, and carbonization temperature were 0.1 g, 75 mg/L, 60 min, pH 7, 25 mL, and 350 °C, respectively. The equilibrium adsorption isotherms were also examined. The Langmuir and Freundlich adsorption models were used to examine the experimental data. The greatest quantity of MB that could adsorb on the FGAC surface was 65 mg/g, as predicted by the Langmuir model.

*Corresponding Author:
Fouad Fadhil Al-Qaim
E-mail: fouad.fadhil@uobabylon.edu.iq
Tel.: +09647827744903

KEYWORDS

Response surface methodology; elimination process; cationic dye; cheap adsorbent; adsorption; isotherms.

Introduction

Several life forms have had major issues as a result of dye effluents released by textile and industrial effluents, and the environment over the last few decades. Since most of these colors are unhealthy and can irritate skin and trigger allergies, it is imperative from a health standpoint to remove dyes from the aquatic environment. Most of these dyes are mutagenic and carcinogenic [1-3]. Thus, prior to go out into the surroundings, each dye found in the sample have to be treated [4,5]. Methylene blue, one of the most well-

J. Med. Pharm. Chem. Res.5 (2023) 794-811

P a g e | **794**

known dyes, is more frequently employed in cotton and wood coloring [6].

A few of the negative effects that MB can have on people include elevated heart rate, vomiting, shock, the development of Heinz bodies, cyanosis, jaundice, quadriplegia, and tissue necrosis [7]. The elimination of such a color from process effluent is therefore crucial for the environment. There are numerous treatment techniques available to remove colors from wastewater. These techniques include cation exchange membranes [8], electrochemical oxidation [9], electrochemical-coagulation [10], photocatalytic oxidation [11], Fenton-chemical degradation [12,13], and biotreatment [14-16]. When compared to other water treatment techniques, adsorption is one of the more promising ones for removing colors from water solutions [17].

The adsorption procedure has more benefits than other techniques, such as an elevated potential for dye removal, superior production mobility, a straightforward design, and gratifying performance [18]. To remove colors from wastewater, activated carbon (AC) adsorption is now the most often used technique [19]. Using agricultural waste, scientists have been working on developing cheap adsorbents to eliminate many toxins out of real samples during the last few years. Natural wastes has been used to form activated carbon, it has the advantages of being renewable, biodegradable, and environmentally friendly [20-29].

Some studies suggest that inexpensive adsorbents for dye removal from wastewater can be made using agricultural byproducts like durian shells, mango seed kernel powder, and grape stalks. These goods include grape stalks [30], powdered mango seed kernels, and durian shells [31].

This investigation looked at the removal of methylene blue (MB) from aqueous solutions using activated carbon made from discarded fig leaves. To create the ideal environment for MB elimination, duration, actual level of MB, dosage, sample volume, agitation time, carbonization temperature, and pH solution were examined using Box-Behnken Design (BBD-RSM) through the response surface methodology. SEM and FT-IR analyses were used to examine the prepared activated carbon's physical and chemical characteristics. The characteristics of MB adsorption on carbon-based surfaces was then investigated while taking into account the adsorption mechanism using isotherm and kinetics investigations.

Experimental

Material and methods

The fig leaves utilized in this study were gathered from vineyards in the Iraqi province of Babylon. Fig leaves were washed in distilled water then left for one night. After that, it was crushed and sieved through a 75-mesh. H_3PO_4 was supplied by Merck to operate as an activator. The adsorbate model used in adsorption research is the basic (cationic) dye methylene blue ($C_{16}H_{18}ClN_3S$), which was bought from Dyestuffs and Chemicals Co. (China). Only chemicals of the analytical grade were used, and no additional steps were necessary.

Activated carbon preparation

The fig leaves were gathered crisp, or dry, and then immersed in water to eliminate the solid matters before drying. The fig leaves were then ground with an electric grinder and sieved through a 75-mesh screen. The beaker with the 3 g of powdered fig leaves received 10 mL of deionized water. After that, 2.5 mL of concentrated H_3PO_4 was added separately and constantly mixed until the powder was well dissolved. After being left for two hours, it was thoroughly rinsed with water to get the pH down to 6.7, and then the sample was dried naturally for one

or two nights. Carbonization step has applied on the dried sample at 150, 350, and 550 °C for 120 min.

Adsorption experiments

The sample MB concentrations (20, 62.5, and 100 mg/L) were mixed with various amounts of adsorbent (0.02, 0.06, and 0.1 g), and the mixture was agitated for 20, 40, and 60 minutes at the ambient temperature.

$$R\% = \frac{C_0 - C_t}{C_0} \times 100 \tag{1}$$

$$Q = \frac{(C_0 - C_t)}{m} \times V \tag{2}$$

Where, C_t is the MB concentration (mg/L) after a specific amount of time and C_0 is the initial MB concentration (mg/L).

Following the adsorption process, R% is the MB percentage that has been removed, Q is the adsorption ability (mg/g), and m is the amount of fig activated carbon (g). To generate the required pigment solutions, stock MB solution (1000 mg/L) was dissolved in double-distilled water. The calibration curve for the UV-Vis spectrophotometer shows that adsorbent was added in amounts of 25, 62.5, and 100 mL of MB solution with a wide range of concentrations (20, 60, and 100 mg/L) and 0.02, 0.06, and 0.1 g. A 20-100 mg/L concentration of MB dye and pH values of (3, 7, and 11) were used to show the effects of pH.

Experimental design

Using mathematical and statistical analysis, RSM is a technique for creating empirical models used to optimize removal% impacted by a number of different input variables. Using the fewest possible experimental runs in accordance with the experimental design, RSM develops the regression model equation and the optimum conditions [32-35]. For the

During the adsorption, the samples were centrifuged at 3000 rpm, and the resulting filtrates were analyzed. The MB dye's maximum wavelength was measured using a UV-Vis spectrophotometer to be 654 nm. After the adsorption process was subjected to the calibration curve, the MB concentrations were monitored. The removing percent and ability to adsorb of the MB dye were determined using Equations (1, 2):

current job, a Box-Behnken Design software was utilized. This rotatable design typically works well for process optimization and is appropriate for fitting a quadratic surface [11]. We chose six independent variables, including starting MB concentration (A), adsorbent dosage (B), pH (C), carbonization temperature (D), volume of solution (E), and agitation time (F), to assess the impact of operating variables on dye removal (Y). For six variables, 108 runs were conducted using Box-Behnken Design software.

Batch experiments

Studies on the elimination of methylene blue were conducted by modifying the BBD process settings. The FGAC adsorbent dosages were 0.02-0.1 g, the beginning MB concentration was 20-100 mg/L, the initial pH of the MB solution was 3-11, the carbonization temperature was 150-550 °C, the sample volume was 25-100 mL, and the contact periods were 20-60 min. A shaker device has set to 120 rpm was used to agitate the flasks at room temperature (RT = 22±2 °C) while the appropriately weighed adsorbent FGAC powder was introduced. After a predetermined amount of time, samples were taken, centrifuged, filtered

through a nylon syringe filter (Whatman; pore size: 0.2 mm, diameter: 25 mm), and then examined using a UV-Vis spectrophotometer with a max wavelength of 654 nm.

Results and discussion

Fourier transform infrared spectroscopy

The presence of the principal functional groups on the exterior of the biosorbent can be qualitatively evaluated using Fourier transform infrared spectroscopy (FTIR). The most importance functional groups are hydroxyl groups, carbonyl groups, and so on [36-39]. Figure 1 examines the FTIR of adsorbent surface. It is possible that the vibrations of hydroxyl functional groups are what are causing the signal at 3065 cm^{-1}. The carbonyl group C=O [40] is vibratory stretched as shown by the bands at 1622 cm^{-1}. The C-O band, which has a significant resonance at 1317 cm^{-1}, lost some of its intensity.

Scanning electron microscopy

It was observed that activating of the carbon surface resulted many holes [41]. These sites help to track the MB molecules, as demonstrated in the Figure 1b.
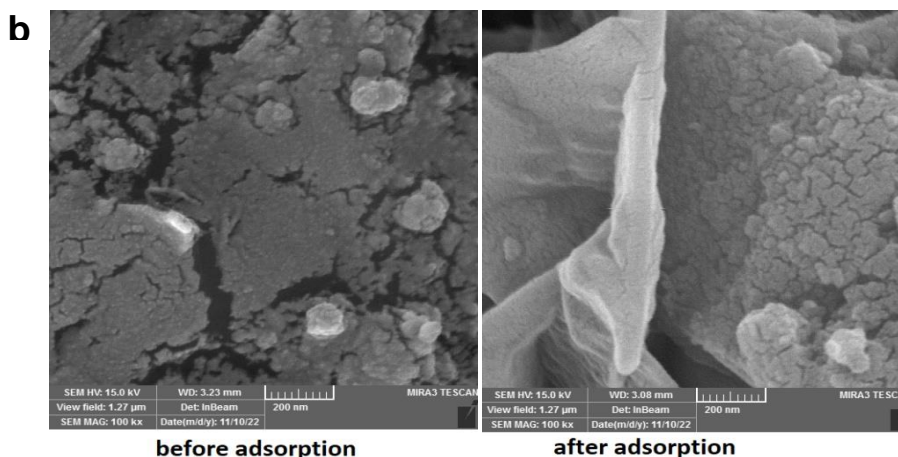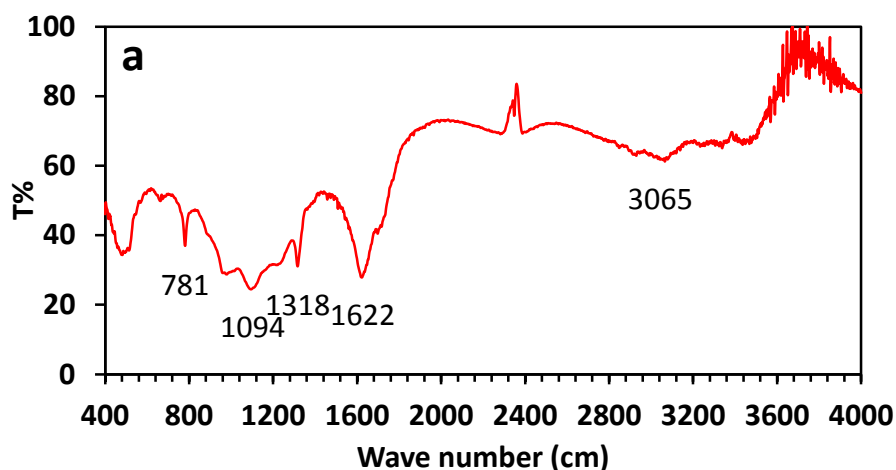

FIGURE 1 Intensities of the most prevalent functional groups for FGAC discovered using FTIR; (a) photographs of FGAC before and (b) after adsorption

Statistical analysis

A 108 runs produced by the Box-Behnken Design software, the six distinct process factors, including initial MB level (A), dose of adsorbent (B), pH (C), carbonizing temperature (D), the solution volume (E), and contact period (F), and their dynamic impacts on the MB removal rate (as removal%), were examined.

Model validation

An analysis of variance (ANOVA) was utilized to assess the statistical importance of the RSMD model. The results of the second-order interaction surface model are presented as an ANOVA in Table 1. Model terms with P 0.05 values demonstrate that certain circumstances make particular factors as the significant model parameters for responding (MB removal %) included and (A2 to F2 except C2).

TABLE 1 Analysis of variance

Source	DF	Sum of squares	Mean square	F-value	P-value
Model	27	58711.4	2174.5	35.55	0.000
Linear	6	49390.6	8231.8	134.57	0.000
A	1	1142.7	1142.7	18.68	0.000
B	1	11297.6	11297.6	184.68	0.000
C	1	132.7	132.7	2.17	0.145
D	1	639.5	639.5	10.45	0.002
E	1	34797.9	34797.9	568.84	0.000
F	1	1380.3	1380.3	22.56	0.000
A2	1	801.1	801.1	13.10	0.001
B2	1	502.6	502.6	8.22	0.005
C2	1	15.4	15.4	0.25	0.618
D2	1	1014.4	1014.4	16.58	0.000
E2	1	1988.6	1988.6	32.51	0.000
F2	1	331.0	331.0	5.41	0.023
AB	1	2.3	2.3	0.04	0.848
AC	1	60.1	60.1	0.98	0.325
AD	1	4.2	4.2	0.07	0.794
AE	1	2.6	2.6	0.04	0.838
AF	1	720.9	720.9	11.78	0.001
BC	1	302.8	302.8	4.95	0.029
BD	1	210.3	210.3	3.44	0.067
BE	1	2872.8	2872.8	46.96	0.000
BF	1	42.3	42.3	0.69	0.408
CD	1	98.0	98.0	1.60	0.209
CE	1	376.4	376.4	6.15	0.015
CF	1	55.7	55.7	0.91	0.343
DE	1	557.0	557.0	9.10	0.003
DF	1	1.2	1.2	0.02	0.889
EF	1	125.4	125.4	2.05	0.156
Error	80	4893.8	61.2		
Lack-of-Fit	21	4891.8	232.9	6871.88	0.000
Pure Error	59	2.0	0.0		
Total	107	63605.2			

Also, significant within (P<0.05) are the other two-way variables (AE, BE, BC, EC, and DE). Thus, the equation created is written as follows:

S.T. Al-Asadi and F.F. Al-Qaim

$$
\begin{aligned}
\text{Removal\%} = \ & 83.7 - 1.366\,A + 1008\,B - 2.19\,C + 0.1945\,D - 1.345\,E \\
& + 0.209\,F + 0.00998\,C2 - 3089\,B2 - 0.054\,C2 - 0.000176\,D2 + 0.00699\,E2 \\
& + 0.01003\,F2 + 0.38\,AB + 0.0194\,AC \\
& + 0.000073\,AD + 0.00043\,AE - 0.01343\,AF + 27.2\,BC - 0.453\,BD \\
& - 6.317\,BE + 2.03\,BF - 0.00309\,CD + 0.0323\,CE \\
& - 0.0165\,CF - 0.000787\,DE + 0.000069\,DF + 0.00373\,EF \qquad (3)
\end{aligned}
$$

Figure 2 displays the regular likelihood of the residual for MB elimination. The pattern suggests that MB pigment residue behaves itself, is dispersed uniformly, and forms a straight line. In addition, Figure 3 shows residue vs. predicted response. The assumption of constant variance is tested by plotting the residual against the ascending expected response value. The plot's points are dispersed at random, and the residuals' range is constant throughout the graph. According to Figure 3, the residuals in the plot move randomly about the middle line.
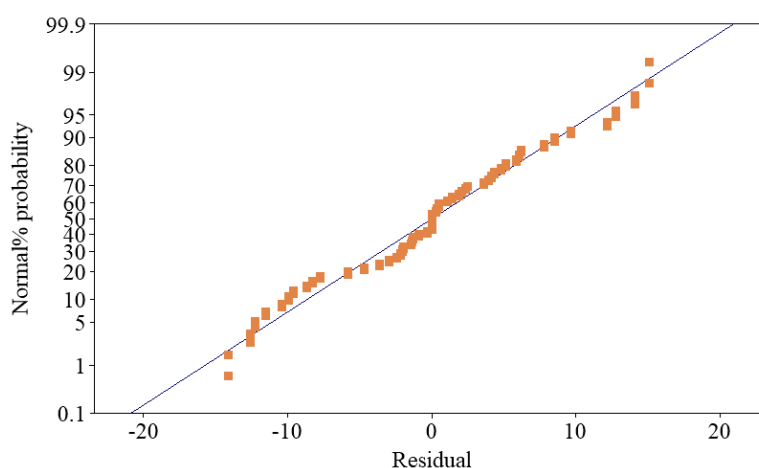

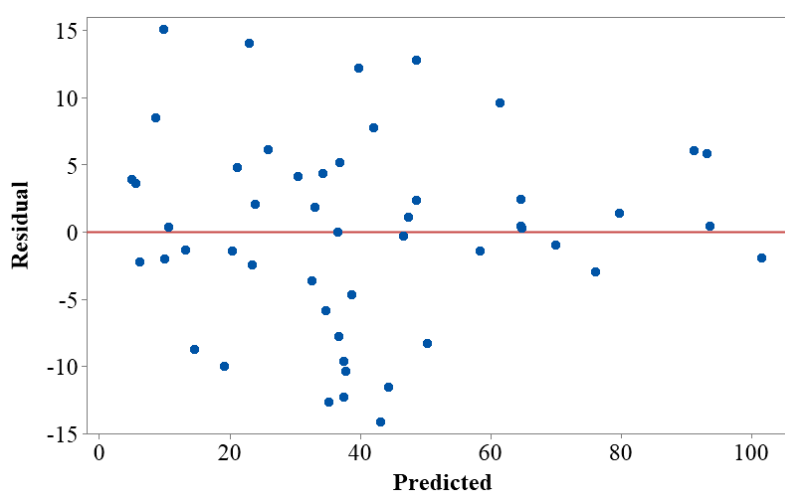**FIGURE 2** Plots of normal probabilities for the elimination efficiency of MB

FIGURE 3 The plot of the residual vs. expected response for adsorption of methylene blue dye on FGAC

Figure 4a shows the normal probability distribution of standardized impacts with p = 0.05 to evaluate the significance of each factor and its effects on the effectiveness of removal (%). The right and left portions of a normal probability plot could be separated. The right region (from B to BC) has positive coefficients, while the left sector (from E to BE) contains negative coefficients. The blue ball's dimensions don't matter. The square-symbolized components are regarded as important. The relative importance of each effect and interaction impacts was shown by the Pareto diagram of the standardized impacts in Figure 4b.

The estimated impacts were tested using the Student's t-test to see if they were statistically different from zero. The values for every impact were shown in the horizontal bars of the Pareto chart. At a 95% confidence level, the straight line in the graph reflects the smallest statistically significant impact value (1.99). On the right side of the solid line, all values greater than 1.99 (p = 0.05) are significant. Each change in the volume of solution and the quantity of adsorbent dose (B) led to an increase in the % removal of MB because the solution volume increased the amount of MB that was present in the solution and was ready for adsorption on FGAC when the adsorbent was increased. Therefore, these factors have a significant impact on increasing the MB elimination. An increase in adsorbent and a decrease in volume jointly led to an increase in removal efficiency (%) because the interaction of two parameters BE gives favorable signal on the removal efficiency of MB. The MB removal procedure' univariate optimization would not be able to distinguish between this antagonistic effect and others.
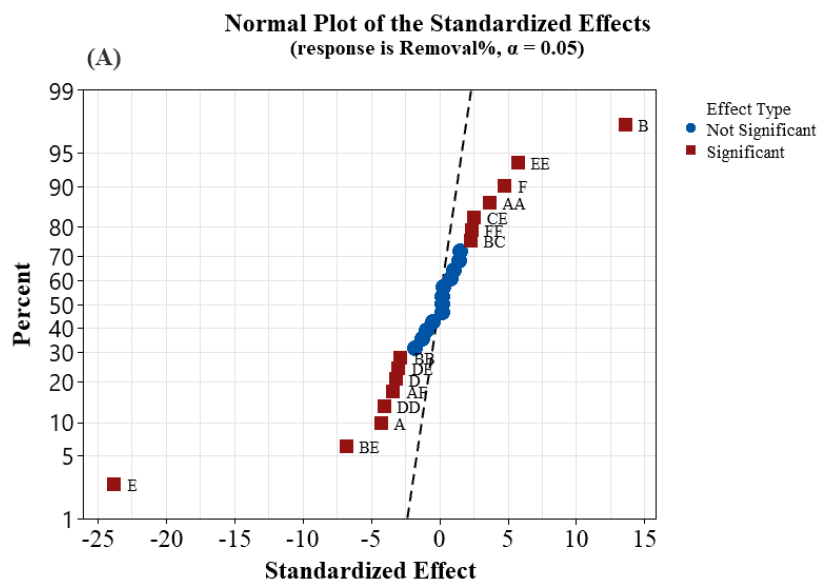

Pareto Chart of the Standardized Effects
(response is Removal%, α = 0.05)
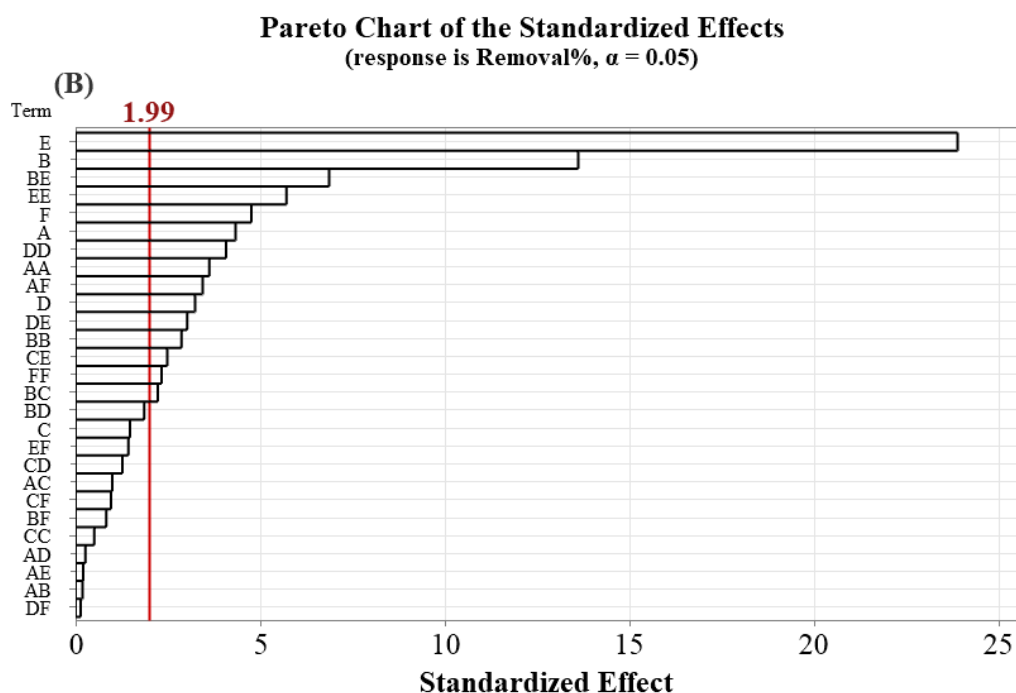
FIGURE 4 (a) normal plot and (b) pareto plot for analysis of removal of methylene blue under optimum conditions

Response interactions along with process improvement

The best rate of MB elimination may be achieved using each of the following association variables, based on Table 1's ANOVA findings for the response variable: AF, BC, BE, CE, and DE. Figures 5-9 display the response's 3D and contour plots for the ideal interaction terms of AF, BC, BE, CE, and DE, respectively, while maintaining the central level constants for other variables.

On the effectiveness of MB removal (response), the combined impact of initial MB concentration (A) and time (F) were statistically significant (p = 0.001, Table 1). Figure 5(a) and (b) show the 3D and contour diagrams of the MB removal rate at 0.06 g, pH 7, 350 °C carbonization temperature, and volume of 25 mL, respectively. Starting MB level is highly efficient in eliminating MB molecules from a specific solution. In contrast, time controls how long the MB saturation lasts on the carbon's surface. Therefore, the interaction effect has an impact on the model. The efficiency of MB removal increased to 94% when concentration was simultaneously reduced and agitation time was lengthened. The adsorption process reached equilibrium at a concentration of about 50 mg/L and remained steady with increasing time, making this the ideal beginning concentration. Increasing the initial concentration typically results in a large number of molecules competing for surface adsorptive space, which reduces the adsorption effectiveness. Due to the abundance of MB molecules, which causes the active sites to be saturated quickly with enough MB, low MB removal can be explained at high concentrations.
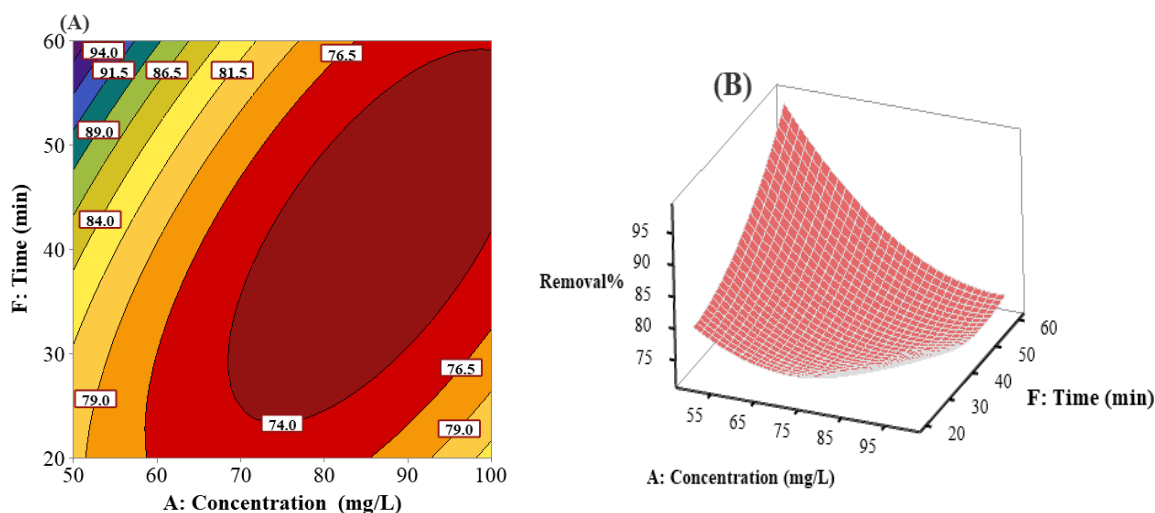
FIGURE 5 The MB effectiveness of elimination contour diagrams (a) and 3D graphs (b) against concentration dye and agitation time at 0.06 g FGAC, 350 °C carbonization temperature, 25 mL solution, and initial pH 7

The efficacy of MB elimination (response) was significantly influenced by the amount of adsorbent (B) and volume (E) combined. The MB elimination effectiveness at 75 mg/L dye level, 350 C carbonization temperature, 40 min of agitation, and the initial pH 7 is shown in the 3D and contour diagrams of Figure 6(a) and (b), respectively. The solution volume provides a better habitat for the FGAC particles and the dye. Combining a reduction in solution volume with an increase in FGAC dosage resulted in an improvement in MB removal effectiveness to 88%. Yet, MB elimination underwent a striking change when the volume was reduced while maintaining a constant FGAC dose. This outcome, which is connected to the quantity of MB molecules present in solution, has already been explored.
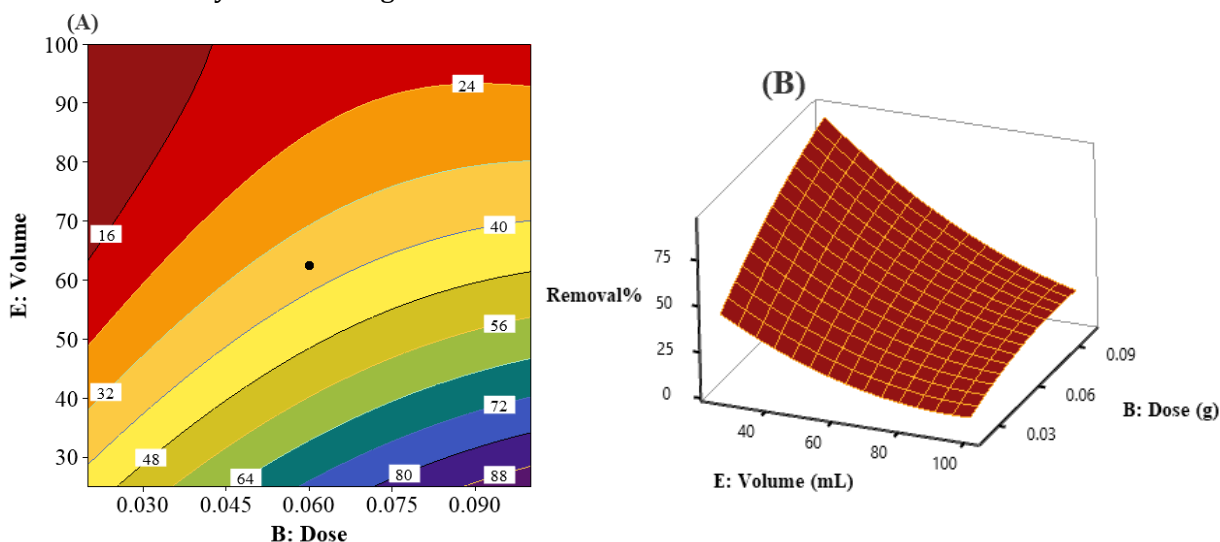

FIGURE 6 The MB effectiveness of elimination contour diagrams (a) and 3D graphs (b) against volume solution and FGAC dose at 75 mg/L dye concentration, 350 °C carbonization temperature, 40 min of agitation time, and initial pH 7

The efficacy of MB elimination at 75 mg/L dye level, 0.06 g dose of FGAC, pH solution of 7, and agitation time of 40 min is shown in the 3D and contour plots of Figure 7. The combined effect of initial volume solution (E) and the carbonization temperature (D) on the effectiveness of MB removal (response) was significant (p = 0.003, Table 1), and the MB removal efficacy at these conditions is shown in the 3D and contour plots. With a concomitant rise in temperature carbonization and decrease in solution volume, MB removal efficiency quickly climbed to 76.5%. More organic material was converted into the activated carbon as a result of high temperature than there were additional sites created on the surface. The MB molecules can therefore live on the surface with respect to these sites.
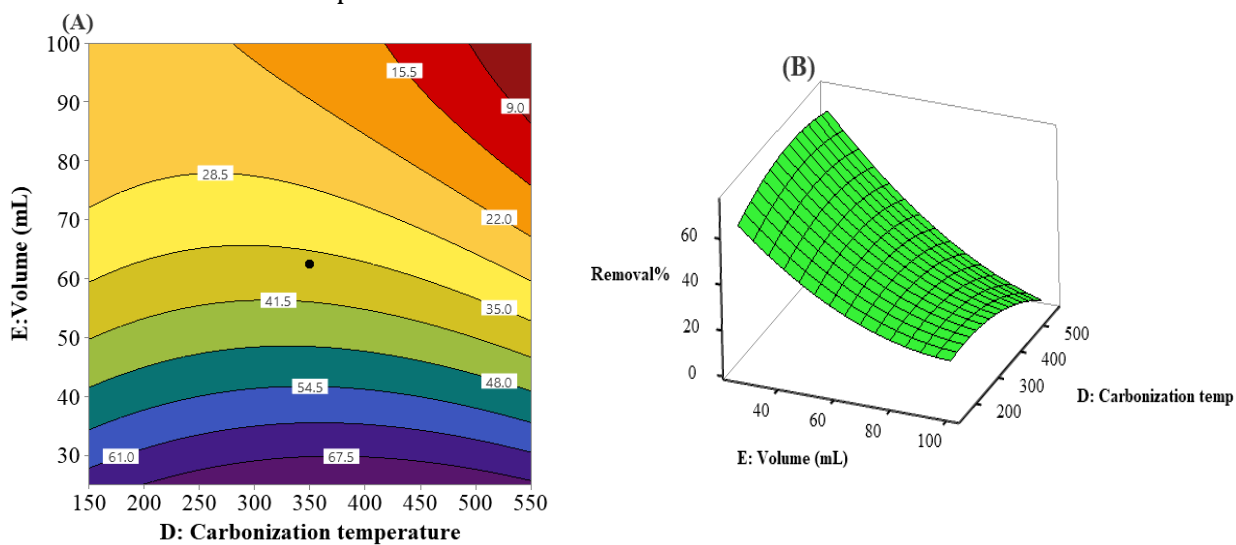

FIGURE 7 The MB effectiveness of elimination contour diagrams (a) and 3D graphs (b) against volume solution and carbonization temperature at 75 mg/L dye concentration, 0.06 g FGAC, 40 min of agitation time, and initial pH 7

A combined impact of starting pH (C) and volume solution (E) on the efficacy of eliminating MB (response) were significant (p = 0.015, Table 1). The three-dimensions and contour charts of Figure 8 depict the MB elimination efficacy at 75 mg/L dye concentration, 0.06 g of FGAC, 350 °C carbonization temperature, and 40 min of agitation. The elimination efficiency of MB in low amounts (30 mL) of acidic solution quickly increased to 72%. The elimination percentage decreased to 18% in the same condition at quantities more than 80 mL, but it was 66 for volumes between 30 and 40 mL with a pH of 10. After that, all accessible adsorption holes on the outer surface of FGAC particles have been occupied for the entire 40-min period, reduced solution volumes give the MB molecules a greater opportunity to access the inside of adsorbent pore.
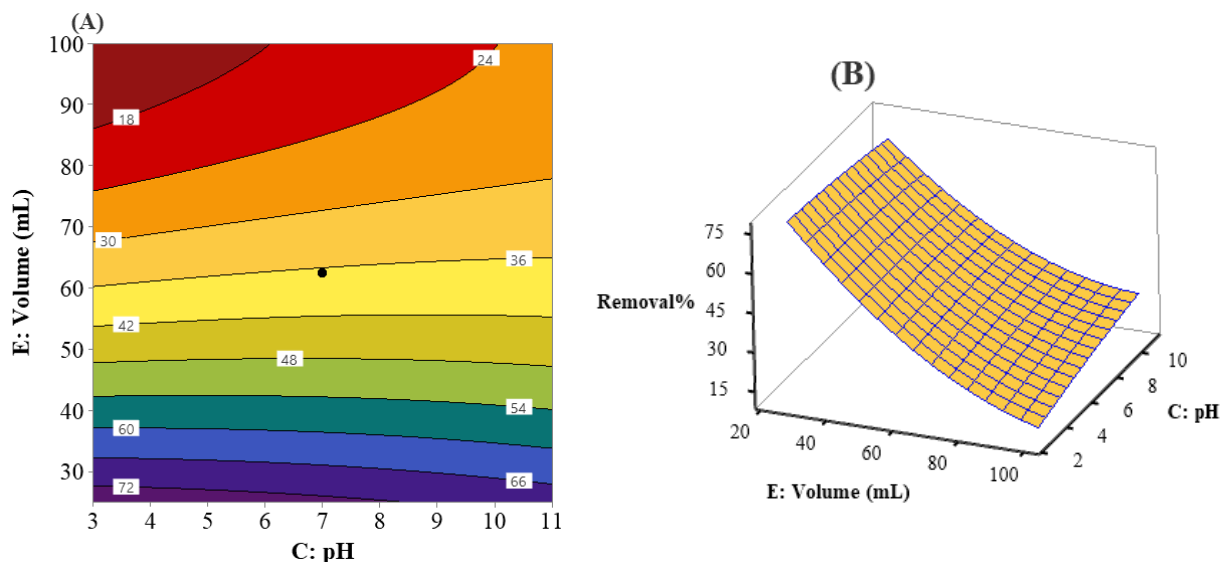
FIGURE 8 The MB effectiveness of elimination contour diagrams (a) and 3D graphs (b) against volume solution and pH solution at 75 mg/L dye concentration, 350 °C carbonization temperature, 40 min of agitation time, and 0.06 g of FGAC

According to Figure 9, the optimal FGAC dose was roughly 0.1 g since at this dosage; the adsorption mechanism reached equilibrium and remained steady as the FGAC mass increased. Increasing the adsorbent dosage often results in more surface area and more binding sites being available [42]. Even though the solution is still basic, very low levels of MB removal were seen at low adsorbent doses at the same time.

Low elimination of MB at acidic pH levels can be due to the existence of H_3O^+ ions, which compete with the dye cations for adsorption sites. The advantage of an adsorbent is that it may decolorize real textile industry effluent, which is naturally alkaline, without incurring extra costs due to pH regulation [43]. Similar behavior was seen when MB was extracted using several carbon adsorbent materials [44-47].
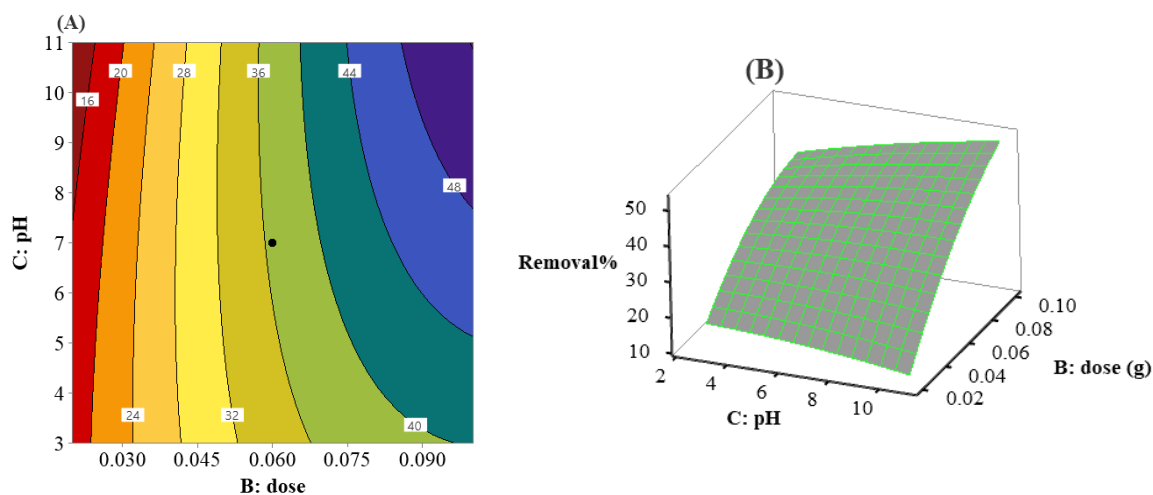

FIGURE 9 The MB effectiveness of elimination contour diagrams (a) and 3D graphs (b) against pH solution and FGAC dose at 75 mg/L dye concentration, 350° C carbonization temperature, 40 min of agitation time, and 62.5 mL solution

Adsorption isotherm studies

According to the Langmuir model, adsorptions take place at predetermined homogenous sites on the adsorbent. Many monolayer adsorption methods use this

$$\frac{C_e}{Q_e} = \frac{1}{Q_{max}K_L} + \frac{1}{Q_{max}}C_e \qquad (4)$$

The exterior homogeneity of the adsorbent is shown in Figure 10 by the Langmuir-type adsorption isotherm. Small adsorption patches that essentially perform the same adsorption processes as one another make up the adsorbent surface.

paradigm with success [49]. The findings from equilibrium experiments for the sorption of MB dye over FGAC may match the Langmuir equation, which includes the following information:

The adsorption results for the MB dye onto FGAC are shown to fit the Langmuir isotherm with a correlation factor (R2) value of 0.9995. Table 2 presents the results of calculating the values for the constants KL and b.
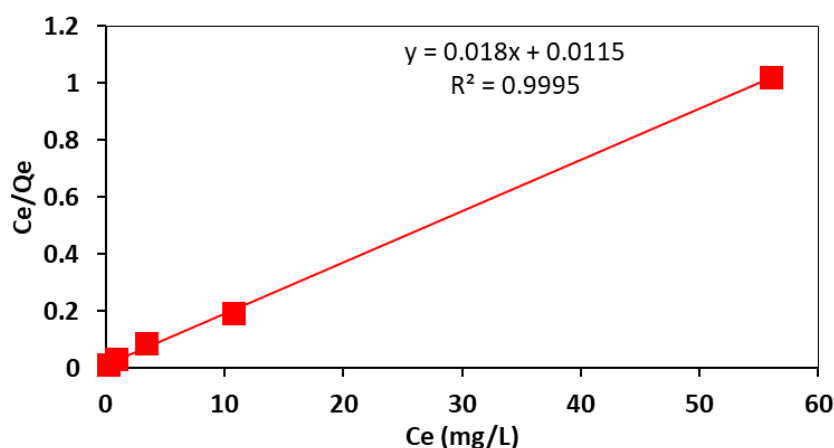

FIGURE 10 Isotherm graphs for MB absorption on FGAC show Langmuir data

Freundlich model

On homogeneous surfaces, the Freundlich model can be applied to non-ideal and

$$\ln Q_e = \ln K_f + \frac{1}{n}\ln C_e \qquad (5)$$

Where, KF is the Freundlich equilibrium a constant, n is an empirical number, and all other terms have their usual meanings. As a

multilayer adsorption processes (41). The following framework is provided as follows:

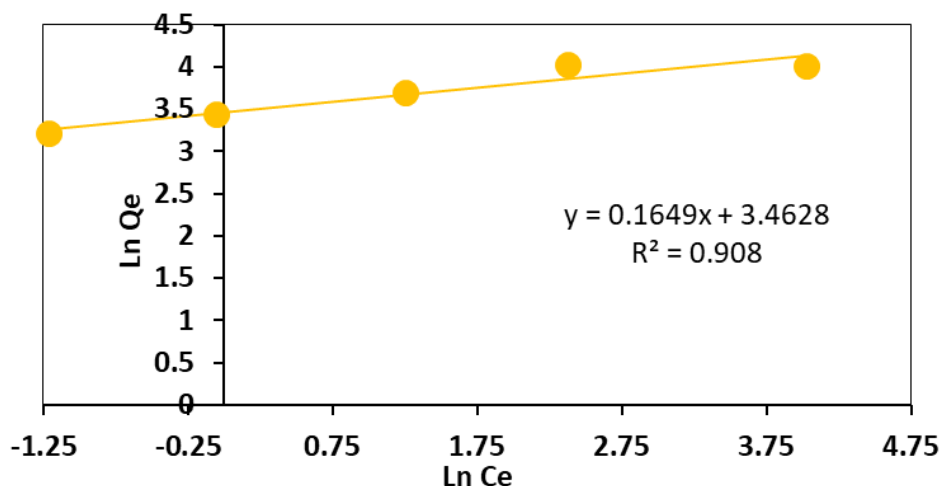result, a plot of ln qe vs. ln Ce was presented in (Figure 11 and Table 2).

FIGURE 11 Isotherm plots Freundlich for MB adsorption on FGAC

TABLE 2 Langmuir and Feruindlich parameters

Isotherm	Parameter	Value
Langmuir	Q_m	65
	K_L	0.08
	R^2	0.9995
Feruindlich	K_F	31.9
	N	6.06
	R^2	0.9080

The high correlation factor for the model was (0.9995) in comparison to the Freundlich (0.9080) model supports this conclusion. As a result, the MB adsorption on FGAC takes place as monolayer adsorption on a surface with a uniform adsorption affinity. The estimated Q_{max} of FGAC for MB was 65 mg/g for monolayer adsorption. The FGAC adsorbent's maximum sorption capacity (Q_{max}) for MB was compared to that for several adsorbents/MB adsorption systems, as described in the literature (Table 3).

TABLE 3 Experimental conditions and the maximum adsorption capacity for numerous leaves waste materials as low cost adsorbents compared with FGAC

Leaves-source	Reagent used	MB Conc. (mg/L)	AC/solution (g/mL)	Treatment time (min)	(Q_{max}) mg/g	References
Fig leaf	H3PO4	80 mg/L	0.8/25	60 min	65 mg/g	The present study
Pineapple leaf	ZnCl2 500 °C	50 mg/L	0.5/50	15 min	288.34 mg/g	[51]
Grape leaf	No reagents (500 °C for 2 hours)	100 mg/L	1.25/100	90 min	[a]0.2 mg/L	[52]
Enset leaf	HCl (no carbonization)	10 mg/L	2.5/1000	60 min	35.5 mg/g	[53]

Journal of Medicinal and Pharmaceutical Chemistry Research

Banana leaves	H_3PO_4 (450, 550 and 600 °C)	2.5 mg/L	0.0035/25	60 min	19-48 mg/g	[54]
Agave salmiana leaves	H_3PO_4 (500 °C for 4 hours	50 mg/L	0.2/50	180 min	95.5 mg/g	[55]
Sugarcane leaves	CH3COOH/H_2O_2 70:30	300 mg/L	0.4/50	300 min	36.5 mg/g	[56]

[a]It was written as it.

Conclusion

The feasibility of adsorbing MB onto fallen fig leaves, a typical agricultural waste in Iraq, was investigated in this work. The ideal adsorption conditions, which comprise the amount of adsorbent, initial MB level, pH, and agitation time, can be found using RSM. The findings suggest that falling FGAC may be used to remove lead basic dye (MB) from aqueous solution. Longer contact times, higher pH values, and higher starting dye levels led to an increase in the quantity of MB dye uptake (mg/g). These equilibrium results supported the single-layer ability to adsorb of the MB pigment onto FGAC with a monolayer sorption capacity of 65 mg/g, which suited the Langmuir isotherm equation. Our findings show that employing dropping FGAC to eliminate basic dye from water-based solutions is practical and affordable.

Acknowledgements

Conflict of Interest

The authors declare no conflict of interest.

Orcid:

Safaa Talib Al-Asadi:
https://orcid.org/0009-0006-4914-7339
Fouad Fadhil Al-Qaim:
https://orcid.org/0000-0002-3473-4980

References

[1] R.O.A. de Lima, A.P. Bazo, D.M.F. Salvadori, C.M. Rech, D. de Palma Oliveira, G. de Aragão Umbuzeiro, Mutagenic and carcinogenic potential of a textile azo dye processing plant effluent that impacts a drinking water source, *MRGTEM*, **2007**, *626*, 53-60. [crossref], [Google Scholar], [Publisher].

[2] M.S. Tsuboy, J.P.F. Angeli, M.S. Mantovani, S.Knasmüller, G.A. Umbuzeiro, L.R. Ribeiro, Genotoxic, mutagenic and cytotoxic effects of the commercial dye CI Disperse Blue 291 in the human hepatic cell line HepG2, *Toxicology in vitro*, **2007**, *21*, 1650-1655. [crossref], [Google Scholar], [Publisher].

[3] R. Caritá, M.A. Marin-Morales, Induction of chromosome aberrations in the Allium cepa test system caused by the exposure of seeds to industrial effluents contaminated with azo dyes, *Chemosphere*, **2008**, *72*, 722-725. [crossref], [Google Scholar], [Publisher].

[4] F.A. Pavan, S.L. Dias, E.C. Lima, E.V. Benvenutti, Removal of Congo red from aqueous solution by anilinepropylsilica xerogel, *Dyes and Pigments*, **2008**, *76*, 64-69. [crossref], [Google Scholar], [Publisher].

[5] F.A. Pavan, Y. Gushikem, A.C. Mazzocato, S.L. Dias, E.C. Lima, Statistical design of experiments as a tool for optimizing the batch conditions to methylene blue biosorption on yellow passion fruit and mandarin peels, *Dyes and Pigments*, **2007**, *72*, 256-266. [crossref], [Google Scholar], [Publisher].

[6] B.H. Hameed, A.L. Ahmad, K.N.A. Latiff, Adsorption of basic dye (methylene blue)

onto activated carbon prepared from rattan sawdust, *Dyes and pigments*, **2007**, *75*, 143-149. [crossref], [Google Scholar], [Publisher].

[7] P.S. Kumar, S. Ramalingam, K. Sathishkumar, Removal of methylene blue dye from aqueous solution by activated carbon prepared from cashew nut shell as a new low-cost adsorbent, *Korean J. Chem. Eng.*, **2011**, *28*, 149-155. [crossref], [Google Scholar], [Publisher].

[8] J.S. Wu, C.H. Liu, K.H. Chu, S.Y. Suen, Removal of cationic dye methyl violet 2B from water by cation exchange membranes, *J. Membr. Sci.*, **2008**, *309*, 239-245. [crossref], [Google Scholar], [Publisher].

[9] L. Fan, Y. Zhou, W. Yang, G. Chen, F. Yang, Electrochemical degradation of aqueous solution of Amaranth azo dye on ACF under potentiostatic model, *Dyes and pigments*, **2008**, *76*, 440-446. [crossref], [Google Scholar], [Publisher].

[10] P. Cañizares, F. Martínez, C. Jiménez, J. Lobato, M.A. Rodrigo, Coagulation and electrocoagulation of wastes polluted with dyes, *Environ. Sci. Technol.*, **2006**, *40*, 6418-6424. [crossref], [Google Scholar], [Publisher].

[11] A.H. Jawad, A.F. Alkarkhi, N.S.A. Mubarak, Photocatalytic decolorization of methylene blue by an immobilized TiO2 film under visible light irradiation: optimization using response surface methodology (RSM), *Desalination Water Treat.*, **2015**, *56*, 161-172. [crossref], [Google Scholar], [Publisher].

[12] Y.S. Woo, M. Rafatullah, A.F.M. Al-Karkhi, T.T. Tow, Removal of Terasil Red R dye by using Fenton oxidation: a statistical analysis, *Desalination Water Treat.*, **2014**, *52*, 4583-4591. [crossref], [Google Scholar], [Publisher].

[13] A.R. Khataee, M. Safarpour, A. Naseri, M. Zarei, Photoelectro-Fenton/nanophotocatalysis decolorization of three textile dyes mixture: response surface modeling and multivariate calibration procedure for simultaneous determination, *J. Electroanal. Chem.*, **2012**, *672*, 53-62. [crossref], [Google Scholar], [Publisher].

[14] M.M. El-Sheekh, M.M. Gharieb, G.W. Abou-El-Souod, Biodegradation of dyes by some green algae and cyanobacteria, *Int. Biodeterior. Biodegradation*, **2009**, *63*, 699-704. [crossref], [Google Scholar], [Publisher].

[15] A.R. Khataee, A. Movafeghi, S. Torbati, S.S. Lisar, M. Zarei, Phytoremediation potential of duckweed (Lemna minor L.) in degradation of CI Acid Blue 92: Artificial neural network modeling, *Ecotoxicol. Environ. Saf.*, **2012**, *80*, 291-298. [crossref], [Google Scholar], [Publisher].

[16] Ref 24-RSM followed- 10: A. R. Khataee, G. Dehghan, M. Zarei, E. Ebadi, M. Pourhassan, Neural network modeling of biotreatment of triphenylmethane dye solution by a green macroalgae, *Chem. Eng. Res. Des.*, **2011**, *89*, 172-178. [crossref], [Google Scholar], [Publisher].

[17] J. Mittal, V. Thakur, A. Mittal, Batch removal of hazardous azo dye Bismark Brown R using waste material hen feather, *Ecol. Eng.*, **2013**, *60*, 249-253. [crossref], [Google Scholar], [Publisher].

[18] A. Seidmohammadi, G. Asgari, M. Leili, A. Dargahi, A. Mobarakian, Effectiveness of quercus branti activated carbon in removal of methylene blue from aqueous solutions, *Arch. Hyg. Sci.*, **2015**, *4*, 217-225. [crossref], [Google Scholar], [Publisher].

[19] T. Robinson, B. Chandran, P. Nigam, Effect of pretreatments of three waste residues, wheat straw, corncobs and barley husks on dye adsorption, *Bioresour. Technol.*, **2002**, *85*, 119-124. [crossref], [Google Scholar], [Publisher].

[20] K.S. Hameed, P. Muthirulan, M.M. Sundaram, Adsorption of chromotrope dye onto activated carbons obtained from the seeds of various plants: equilibrium and kinetics studies, *Arab. J. Chem.*, **2017**, *10*, S2225-S2233. [crossref], [Google Scholar], [Publisher].

[21] E.F. Olasehinde, S.M. Abegunde, Adsorption of methylene blue onto acid

modified raphia taedigera seed activated carbon, *Adv. J. Chem. A*, **2020**, *3*, 663-679. [crossref], [Google Scholar], [Publisher].

[22] Z. Rezayati Zad, B. Moosavi, A. Taheri, Synthesis of monodisperse magnetic hydroxyapatite/Fe$_3$O$_4$ nanospheres for removal of Brilliant Green (BG) and Coomassie Brilliant Blue (CBB) in the single and binary systems, *Adv. J. Chem. Sect. B. Nat. Prod. Med. Chem.*, **2020**, *2*, 159-171. [crossref], [Google Scholar], [Publisher].

[23] N. Odogu Ankoro, R.B. Ngouateu Lekene, J.N. Ndi, D. Kouotou, H.M. Ngomo, J.M. Ketcha, Highly microporous activated carbons from Mangifera indica residues: Optimization of preparation conditions using response surface methodology, *Asian J. Green Chem.*, **2022**, *6*, 1-13. [crossref], [Pdf], [Publisher].

[24] A.M. Al-Layla, A.B. Fadhil, Removal of calcium over apricot shell derived activated carbon: kinetic and thermodynamic study, *Chem. Methodol.*, **2022**, *6*, 10-23. [crossref], [Pdf], [Publisher].

[25] V. Khakyzadeh, H. Rezaei-Vahidian, S. Sediqi, S.B. Azimi, R. Karimi-Nami, Programming adsorptive removal of organic azo dye from aqueous media using magnetic carbon nano-composite, *Chem. Methodol.*, **2021**, *5*, 324-330. [crossref], [Google Scholar], [Publisher].

[26] S.M. Abegunde, K.S. Idowu, Enhanced adsorption of methylene blue dye from water by alkali-treated activated carbon, *Eurasian J. Sci. Technol.*, **2023**, 109-124. [crossref], [Pdf], [Publisher].

[27] S. Gaikwad, M. Gaikwad, P. Lokhande, Iodine-DMSO catalyzed aromatization of polysubstituted cyclohexanone derivatives; an efficient methods for the synthesis of polyfunctionized biaryls derivatives, *J. Appl. Organomet. Chem.*, **2021**, *1*, 1-8. [crossref], [Google Scholar], [Publisher].

[28] A. Alkherraz, A. Ali, K. Elsherif, Equilibrium and thermodynamic studies of Pb(II), Zn(II), Cu(II) and Cd(II) adsorption onto mesembryanthemum activated carbon, *J. Med. Chem. Sci.*, **2020**, *3*, 1-10. [crossref], [Google Scholar], [Publisher].

[29] L.S. Muhammed, Removal of nickel(II) by silica aerogel-activated carbon nanocomposite from wastewater, *J. Med. Chem. Sci.*, **2023**, *6*, 2140-2153. [crossref], [Pdf], [Publisher].

[30] B.H. Hameed, F.B.M. Daud, Adsorption studies of basic dye on activated carbon derived from agricultural waste: Hevea brasiliensis seed coat, *Chem. Eng. J.*, **2008**, *139*, 48-55. [crossref], [Google Scholar], [Publisher].

[31] K.V. Kumar, A. Kumaran, Removal of methylene blue by mango seed kernel powder, *Biochem. Eng. J.*, **2005**, *27*, 83-93. [crossref], [Google Scholar], [Publisher].

[32] A. Baçaoui, A. Yaacoubi, A. Dahbi, C. Bennouna, R.P.T. Luu, F.J. Maldonado-Hodar, C. Moreno-Castilla, Optimization of conditions for the preparation of activated carbons from olive-waste cakes, *Carbon*, **2001**, *39*, 425-432. [crossref], [Google Scholar], [Publisher].

[33] Z.R. Holan, B. Volesky, Biosorption of lead and nickel by biomass of marine algae, *Biotechnol. Bioeng.*, **1994**, *43*, 1001-1009. [crossref], [Google Scholar], [Publisher].

[34] M.M.D. Zulkali, A.L. Ahmad, N.H. Norulakmal, L. Oryza sativa husk as heavy metal adsorbent: optimization with lead as model solution, *Bioresour. Technol.*, **2006**, *97*, 21-25. [crossref], [Google Scholar], [Publisher].

[35] C. Cojocaru, G. Zakrzewska-Trznadel, Response surface modeling and optimization of copper removal from aqua solutions using polymer assisted ultrafiltration, *J. Membr. Sci.*, **2007**, *298*, 56-70. [crossref], [Google Scholar], [Publisher].

[36] H.N. Tran, S.J. You, T.V. Nguyen, H.P. Chao, Insight into the adsorption mechanism of cationic dye onto biosorbents derived from agricultural wastes, *Chem. Eng. Commun.*, **2017**, *204*, 1020-1036. [crossref], [Google Scholar], [Publisher].

[37] D. Guo, Y. Li, B. Cui, M. Hu, S. Luo, B. Ji, Y. Liu, Natural adsorption of methylene blue by waste fallen leaves of Magnoliaceae and its repeated thermal regeneration for reuse, *J. Clean. Prod.*, **2020**, *267*, 121903. [crossref], [Google Scholar], [Publisher].

[38] A.H. Jawad, A.R. Ramlah, I. Khudzir, S. Sabar, High surface area mesoporous activated carbon developed from coconut leaf by chemical activation with H_3PO_4 for adsorption of methylene blue, *Desalination Water Treat.*, **2017**, *74*, 326-335. [Google Scholar], [Publisher].

[39] A.K. Kushwaha, N. Gupta, M.C. Chattopadhyaya, Removal of cationic methylene blue and malachite green dyes from aqueous solution by waste materials of Daucus carota, *J. Saudi Chem. Soc.*, **2014**, *18*, 200-207. [crossref], [Google Scholar], [Publisher].

[40] A.S. Abdulhameed, N.N.M.F. Hum, S. Rangabhashiyam, A.H. Jawad, L.D. Wilson, Z.M. Yaseen, Z.A. ALOthman, Statistical modeling and mechanistic pathway for methylene blue dye removal by high surface area and mesoporous grass-based activated carbon using K_2CO_3 activator, *J. Environ. Chem. Eng.*, **2021**, *9*, 105530. [crossref], [Google Scholar], [Publisher].

[41] I. Bencheikh, K. Azoulay, J. Mabrouki, S. El Hajjaji, A. Dahchour, A. Moufti, D. Dhiba, The adsorptive removal of MB using chemically treated artichoke leaves: Parametric, kinetic, isotherm and thermodynamic study, *Sci. Afr.*, **2020**, *9*, e00509. [crossref], [Google Scholar], [Publisher].

[42] M. Kousha, E. Daneshvar, H. Dopeikar, D. Taghavi, A. Bhatnagar, Box–Behnken design optimization of Acid Black 1 dye biosorption by different brown macroalgae, *Chem. Eng. J.*, **2012**, *179*, 158-168. [crossref], [Google Scholar], [Publisher].

[43] G.Z. Kyzas, A decolorization technique with spent "Greek coffee" grounds as zero-cost adsorbents for industrial textile

wastewaters, *Materials*, **2012**, *5*, 2069-2087. [crossref], [Google Scholar], [Publisher].

[44] B.H. Hameed, R.R. Krishni, S.A. Sata, A novel agricultural waste adsorbent for the removal of cationic dye from aqueous solutions, *J. Hazard. Mater.*, **2009**, *162*, 305-311. [crossref], [Google Scholar], [Publisher].

[45] B.H. Hameed, M.I. El-Khaiary, Batch removal of malachite green from aqueous solutions by adsorption on oil palm trunk fibre: equilibrium isotherms and kinetic studies, *J. Hazard. Mater.*, **2008**, *154*, 237-244. [crossref], [Google Scholar], [Publisher].

[46] B.H. Hameed, Removal of cationic dye from aqueous solution using jackfruit peel as non-conventional low-cost adsorbent, *J. Hazard. Mater.*, **2009**, *162*, 344-350. [crossref], [Google Scholar], [Publisher].

[47] L. Kong, L. Gong, J. Wang, Removal of methylene blue from wastewater using fallen leaves as an adsorbent, *Desalination Water Treat.*, **2015**, *53*, 2489-2500. [crossref], [Google Scholar], [Publisher].

[48] H. Lata, V.K. Garg, R.K. Gupta, Removal of a basic dye from aqueous solution by adsorption using Parthenium hysterophorus: an agricultural waste, *Dyes Pigm.*, **2007**, *74*, 653-658. [crossref], [Google Scholar], [Publisher].

[49] I. Langmuir, The adsorption of gases on plane surfaces of glass, mica and platinum, *J. Am. Chem. Soc.*, **1918**, *40*, 1361-1403. [crossref], [Google Scholar], [Publisher].

[50] H. Freundlich, Über die adsorption in lösungen, *Z. Phys. Chem.*, **1907**, *57*, 385-470. [crossref], [Google Scholar], [Publisher].

[51] M.N. Mahamad, M.A.A. Zaini, Z.A. Zakaria, Preparation and characterization of activated carbon from pineapple waste biomass for dye removal, *Int. Biodeterior. Biodegradation*, **2015**, *102*, 274-280. [crossref], [Google Scholar], [Publisher].

[52] S.A. Mousavi, A. Mahmoudi, S. Amiri, P. Darvishi, E. Noori, Methylene blue removal using grape leaves waste: optimization and modeling, *Appl. Water Sci.*, **2022**, *12*, 112. [crossref], [Google Scholar], [Publisher].

Journal of Medicinal and Pharmaceutical Chemistry Research

[53] D. Mekuria, A. Diro, F. Melak, T.G. Asere, Adsorptive removal of methylene blue dye using biowaste materials: barley bran and enset midrib leaf, *J. Chem.*, **2022**. [crossref], [Google Scholar], [Publisher].

[54] M.A. Martín-González, P. Susial, J. Pérez-Peña, J.M. Doña-Rodríguez, Preparation of activated carbons from banana leaves by chemical activation with phosphoric acid. Adsorption of methylene blue, *Revista mexicana de ingeniería química*, **2013**, *12*, 595-608. [Google Scholar], [Publisher].

[55] R.A. Canales-Flores, F. Prieto-García, Taguchi optimization for production of activated carbon from phosphoric acid impregnated agricultural waste by microwave heating for the removal of methylene blue, *Diam. Relat. Mater.*, **2020**, *109*, 108027. [crossref], [Google Scholar], [Publisher].

[56] V. Halysh, O. Sevastyanova, S. Pikus, G. Dobele, B. Pasalskiy, V.M. Gun'ko, M. Kartel, Sugarcane bagasse and straw as low-cost lignocellulosic sorbents for the removal of dyes and metal ions from water, *Cellulose*, **2020**, *27*, 8181-8197. [crossref], [Google Scholar], [Publisher].

How to cite this article: Safaa Talib Al-Asadi, Fouad Fadhil Al-Qaim. Application of response surface methodology on efficiency of fig leaf activated carbon for removal of methylene blue dye. *Journal of Medicinal and Pharmaceutical Chemistry Research,* 2023, 5(9), 794-811.